JOURNAL OF GUIDANCE, CONTROL, AND DYNAMICS
Vol. 30, No. 4, July–August 2007

Engineering Notes

ENGINEERING NOTES are short manuscripts describing new developments or important results of a preliminary nature. These Notes should not exceed 2500 words (where a figure or table counts as 200 words). Following informal review by the Editors, they may be published within a few months of the date of receipt. Style requirements are the same as for regular contributions (see inside back cover).

Trim-Reference Functions for Indirect Method of Trajectory Optimization

Roger L. Barron*
Stanardsville, Virginia 22973
and
Cleon M. Chick III†
Charlottesville, Virginia 22901

DOI: 10.2514/1.28725

I. Introduction

THE improved indirect method of air-vehicle trajectory optimization presented in [1] emphasizes use of performance indices that lead to stable, energy-managed, air-vehicle trajectories, governed primarily via necessary conditions of the calculus of variations. The method provides computationally efficient optimization (and ultimately guidance) of nonsteady, two-point boundary-value (TPBV) maneuvers. The performance indices comprise new analytic maneuver-cost functionals that incorporate time-varying trim-condition reference functions and new isoperimetric penalties on costate-variable rates of change. Final-boundary specifications, inequality constraints, and other nonanalytic trajectory requirements are satisfied via costate initializations using multimodal and steepest-descent searches employing predicted final errors.

This Engineering Note presents further development and analysis of the method proposed in the reference and provides new results from simulations of accurate TPBV maneuvers of a notional unmanned air vehicle (UAV) operating within a vertical plane. These results point a way toward 1) fuel savings in thrusted ascents and descents and 2) independent selection of range and final angle of descent (including vertical strike angle) within the maximum-range glide envelope for the UAV used as an impact weapon.

The integrands of the maneuver-cost functionals are weighted sums of $(\alpha - \alpha_{tr})^2$ and $(T - T_{tr})^2$, in which $\alpha(t)$ is the aerodynamic angle of attack, $T(t)$ is net propulsive thrust, and the subscript $()_{tr}$ denotes a trim (static-equilibrium) reference value. The references are functions of time-varying trajectory states; they do not force maintenance of static equilibrium but alter the penalties to assess *incremental* maneuver efforts expended in satisfying trajectory boundary conditions. The weights are constant, positive-definite, reciprocal Lagrange multipliers.

The trim-reference functions are part of the performance index (PI), which should embody relevant concepts of trajectory cost and merit. Historically, analysts used integrand penalties such as T^2 in the PI, implying $T = 0$ was the reference, that is, that ballistic motion had merit. But, to satisfy final-boundary physical requirements, this meant that the costates (mathematical variables used during indirect optimization as surrogates for missing future states) must grow exponentially in their magnitudes with passage of time, creating acute sensitivity to initial costate settings. Barron and Chick [1] proposed use of trim-reference functions partly to facilitate the stabilization of costates. However, particularly if cross coupling exists between multiple commands, that is, multiple directly manipulated variables such as α and T, or if approximations are used in the reference functions, a further step (also introduced in [1]) should be taken to assure stable behavior of the system costate variables by introducing PI isoperimetric constraints on costate rates, as discussed next.

The air-vehicle equations of motion are anholonomic constraints on the trajectory solutions; these appear in the performance index integrand as a weighted sum of differential equations, each arranged to have an algebraic value of zero, in which the weights, that is, costates, are bipolar and can vary with time. Inequality constraints, such as hard limits on aerodynamic angles, thrust, and airspeed, are imposed by rejecting all inadmissible solutions during predictions of final errors.

The costates govern behavior of the solution even though they are not physical variables. Nonzero costates produce maneuvering (nontrimmed) flight. As a second part of the improved indirect method presented in the reference, the integrand of the performance index incorporates a weighted sum of squares of costate rates of change, the weights being constant, positive-definite Lagrange multipliers. Barron and Chick [1] show that such constraints lead via the calculus of variations to a requirement for constant costate rates, providing further assurance of stability of the costate system and simplifying propagation of costates between boundaries. In particular, costate reinitialization searches are preferably performed at the final boundary and then, with knowledge of the constant costate rates, final-boundary costates can be propagated instantly to the initial boundary to compute optimum $\alpha(t)$ and $T(t)$ commands. The burden of stepwise back integration of the equations of motion and costate differential equations is thereby avoided.

Any constraint on costates potentially compromises optimality. It is tempting to use less restrictive penalties involving the squares of costate second time derivatives, but doing so would impose substantial analytical and computational burdens. Qualitatively, simulation studies presented herein suggest that the loss in performance using costate-rate penalties is small; certainly it is associated with a significant reduction in computing burden. (Quantitative assessments of performance loss and computing burden are a matter for further research.)

Specification of trim-reference functions is related to the class of maneuvers to be performed. An indirectly optimized trajectory is determined primarily by its required boundary conditions, the selected maneuver-cost functional, and the Lagrange multiplier values. The mapping of final-boundary states into initial costates is often not unique and can be multimodal, complicating direct searches for costate initializations. In particular, some modes may exhibit lower fuel consumption than others. Predictive steepest-descent searches are adequate for adaptive reinitializations within a suitable mode. But a flexible, multimodal search, such as a predictive multiple-thread, accelerated random search [1], is recommended for costate initialization at the start of a maneuver.

Received 5 November 2006; revision received 18 January 2007; accepted for publication 23 February 2007.

*Independent Consultant, 7593 Celt Road. Senior Member AIAA.
†Independent Consultant, 405 Four Seasons Drive.

Table 1 Alternative trim-reference functions

Method	Trim functions[a]
A	$\alpha_{\min} = (mg\cos\theta_{\min})/(C_2\rho V_{\min}^2)$, $V_{\min}^2 = mg[-\sin\theta_{\min} + \sqrt{\sin^2\theta_{\min} + (4C_2/C_1)\cos^2\theta_{\min}}]/(2C_2\rho)$, $T_{\min} = C_1\rho V_{\min}^2 + mg\sin\theta_{\min}$
B	$\alpha_{\text{tr}} = (mg\cos\theta_{\text{tr}})/(C_2\rho V^2)$, $T_{\text{tr}} = C_1\rho V^2 + mg\sin\theta_{\text{tr}}$
C	$\alpha_{\text{tr}} = \sqrt{C_1/(C_2 - C_1)}$, $T = 0$

[a] $\theta_{\min} = \gamma + \alpha_{\min}$, $\theta_{\text{tr}} = \gamma + \alpha_{\text{tr}}$

In general, the dimensionality of the costate initialization or reinitialization process must at least equal that of the predictive-error function. In principle, any or all of the final states can be specified (final mass is typically not stipulated) and thereby participate as independent variables in the predicted-error calculation. In [1], the specified final values for thrusted ascents and descents were altitude and rate of climb; at discrete time points along the trajectory, recursive corrections of extremal paths were made while adjusting as few as two of the final-boundary costates. With prior knowledge of costate rates, the final-time costates were readily backpropagated to the (moving) initial time, and with convergence of costate corrections, both the *path-to-go* PI and the final-boundary error function were minimized. Thus the indirectly developed command functions governing angle of attack and thrust variations contained costate values that were initialized via a prediction/correction algorithm.

The emphasis in this Engineering Note is on refinement and application of trim-reference functions, seen as a central consideration for indirect syntheses of real-time trajectory optimization and related guidance processes. Development of the optimum $\alpha(t)$ and $T(t)$ command functions suitable for maneuvers in a vertical plane, with corresponding costate differential equations and algorithms for costate initialization and costate-rate adaptation, follows substantially the presentation in [1] and is omitted here except for revised trim-reference partial derivatives. Two maneuver categories are investigated in this paper: 1) thrusted fixed-duration altitude-change maneuvers with final altitude and vertical velocity specified, and 2) glide-weapon variable-duration trajectories with final altitude, horizontal position, and horizontal velocity specified. The primary objectives of optimization for these maneuver categories are, for the first, minimization of mass loss (fuel consumption) and, for the second, maximization of glide range consistent with realization of a vertical velocity vector at impact.

Three alternative trim-reference methods are presented, the first two being candidates for the first maneuver category, whereas the third is suitable for the second category:

Method A: The velocity $V_{\min}$ that minimizes thrust required for steady-state flight is computed for given atmosphere density ρ, climb angle γ, and vehicle mass m. An iterative solution is then obtained for the α_{tr} and T_{tr} that produce equilibrium at $V_{\min}$.

Method B: An iterative solution is computed for the α_{tr} and T_{tr} that produce equilibrium at the existing V, which generally does not equal $V_{\min}$.

Method C: Trim α_{tr} is computed for maximum steady-state glide range (with $T = T_{\text{tr}} = 0$).

II. Performance Index and Methods for Trim Computation

Table 1 (compiled from [1,2]), which assumes the angle of attack is small, defines the trim-reference functions considered in this paper. These functions appear within the (PI) [1]

$$J = \int_{t_0}^{t_f}\left[(\alpha - \alpha_{\text{tr}})^2/K_1 + (T - T_{\text{tr}})^2/K_2 + \sum_{n=1}^{5}\left(M\dot{\lambda}_n^2 + \lambda_n f_n\right)\right]\mathrm{d}t \tag{1}$$

in which t_0 (typically zero) and t_f are predetermined initial and final times. λ_n is an element of the costate vector (all costates except λ_3 vary with time), and $f_n = 0$ is an anholonomic subsidiary condition expressing the nth state equation [1]. K_1^{-1}, K_2^{-1}, and M are constant Lagrange multipliers. The objective of optimization is to satisfy boundary conditions at t_0 and t_f with a maneuver that minimizes the total cost J. The penalty on $\dot{\lambda}_n^2$ leads to constant costate rates [1].

For method A, α_{tr} and T_{tr} in Eq. (1) become $\alpha_{\min}$ and $T_{\min}$, representing the values for minimum steady-state thrust required. In Table 1, g is the acceleration of gravity (assumed constant); θ is pitch attitude; $\gamma = \sin^{-1}v/V$; u and v denote horizontal and vertical velocity components, respectively; $V = \sqrt{u^2 + v^2}$; $C_1 = C_A S/2$; $C_2 = C_{N_\alpha} S/2$; S is a reference area; C_A is the vehicle axial force coefficient; and C_{N_α} is the partial derivative with respect to α of the normal force coefficient. For the notional unmanned air vehicle [1], $C_A = 0.025$, $C_{N_\alpha} = 3.0\ \text{rad}^{-1}$, and $S = 35\ \text{m}^2$.

Methods A and B require partial derivatives of the trim-reference functions. (These derivatives are zero in method C.) For method A, the nonzero partial derivatives of $\alpha_{\min}$ and $T_{\min}$ are (provided $\alpha_{\min} \neq 0$)

$$\alpha_{\min_{u,v}} = -E_1\gamma_{u,v}/(E_1 + E_2 - \tan\theta_{\min}) \tag{2}$$

$$T_{\min_{u,v}} = \left\{\frac{C_1 mg}{2C_2}\left[\left(\frac{1 - 4C_2/C_1}{2E_2\cos\theta_{\min}}\right)\sin 2\theta_{\min} - \cos\theta_{\min}\right] + mg\cos\theta_{\min}\right\}\theta_{\min_{u,v}} \tag{3}$$

$$T_{\min_m} = g[\sin\theta_{\min} + C_1\cos\theta_{\min}/(C_2\alpha_{\min})] \tag{4}$$

In the preceding relationships, $\gamma_u = -v/V^2$, $\gamma_v = u/V^2$, and

$$E_1 = \frac{\alpha_{\min}}{\cos^2\theta_{\min}}\left(\frac{\tan\theta_{\min}}{E_2} - 1\right) \tag{5}$$

$$E_2 = \sqrt{\tan^2\theta_{\min} + 4C_2/C_1} \tag{6}$$

For method B,

$$\alpha_{\text{tr}_u} = E_3(-2u\cos\theta_{\text{tr}} + v\sin\theta_{\text{tr}})/V \tag{7}$$

$$\alpha_{\text{tr}_v} = E_3(-u\sin\theta_{\text{tr}} - 2v\cos\theta_{\text{tr}})/V \tag{8}$$

$$\alpha_{\text{tr}_h} = -(\alpha_{\text{tr}}\rho_h/\rho)/(1 + E_4\sin\theta_{\text{tr}}) \tag{9}$$

$$\alpha_{\text{tr}_m} = (E_4/m)/(1 + E_4\sin\theta_{\text{tr}}) \tag{10}$$

$$T_{\text{tr}_u} = 2C_1\rho u + mg(\alpha_{\text{tr}_u} - v/V^2)\cos\theta_{\text{tr}} \tag{11}$$

$$T_{\text{tr}_v} = 2C_1\rho v + mg(\alpha_{\text{tr}_v} + u/V^2)\cos\theta_{\text{tr}} \tag{12}$$

$$T_{\text{tr}_h} = C_1\rho_h V^2 + mg\alpha_{\text{tr}_h}\cos\theta_{\text{tr}} \tag{13}$$

$$T_{\mathrm{tr}_m} = g(\sin\theta_{\mathrm{tr}} + m\alpha_{\mathrm{tr}_m}\cos\theta_{\mathrm{tr}}) \tag{14}$$

wherein

$$E_3 = (E_4/V)/(1 + E_4\sin\theta_{\mathrm{tr}}) \tag{15}$$

$$E_4 = mg/(C_2\rho V^2) \tag{16}$$

III. Simulation Results for Methods A and B (Powered Ascent/Descent)

The trim-reference functions of methods A and B are here compared via simulations of the notional UAV, performing powered ascents and descents between specified boundary states. The optimization procedure of [1] is here used with the method A trim-function partial derivatives of Eqs. (2–6) and the method B derivatives of Eqs. (7–16), the latter constituting a revision of the reference. These partial derivatives appear in the costate differential equations (CDEs) of the variational calculus necessary conditions [1]. In the present study, the PI inverse weights, K_1 and K_2, are 5.0 and 1.0, respectively; these were 1.0 and 0.2 in the reference.

The CDEs are initialized via a 16-thread predictive random search that is accelerated as described in [1]. This costate initialization search (CIS) seeks final error magnitudes of less than 100 m in altitude (10 m in [1]) and, simultaneously, less than 0.5 m/s in altitude rate. Horizontal position and its rate of change are not specified. If the independent threads do not reach the accuracy goal in a maximum of 500 iterations (250 iterations in [1]) per thread, the best initial costate vector is selected from among the 16 candidates. Costate-rate adaptation [1] (CRA) follows at the conclusion of the CIS and periodically thereafter to fine tune the (nominally constant) costate rates; the goal of this adaptation is to achieve predicted final error magnitudes of less than 1.0 m in altitude and 0.1 m/s in altitude rate. (The CRA can also provide in-flight guidance reconfiguration [1].)

Ascent and descent maneuvers of specified durations ($t_f - t_0$) of 600, 900, and 1200 s are simulated, the ascents climbing from 2000 to 6000 m and descents doing the opposite. Simulation results suggest that CIS (preadaptation) predicted errors should be less than approximately $0.5(t_f - t_0)$ m in altitude and $0.005(t_f - t_0)$ m/s in altitude rate for satisfactory operation of the CRA.

The CIS search spaces for methods A and B are multimodal, so that global convergence in a finite number of trials is not guaranteed. When method A is used for the 1200 s ascent and when method B is used for the 600 s descent, the 16 threads often fail to find the globally best mode and must be rerun, frequently several times, using different random number sequences. For other maneuvers, the CIS generally uses fewer than 16 threads to converge to initial costates that yield the best performance. On average, CIS convergence is more rapid for method B; however, trajectories obtained with method A generally consume less fuel.

Judging from CIS behavior, some of the search-space modes are associated with *contrary* trajectories in which a brief descent occurs before a sustained climb or a brief climb occurs before a sustained descent. One may view this contrary motion as a form of nonminimum phase response. The CIS converges more slowly in instances where contrary and noncontrary responses produce almost equivalent total fuel consumption. Ultimately, methods A and B select contrary ascents for all three maneuver durations, i.e., 600, 900, and 1200 s, and contrary descents for durations of 900 and 1200 s.

The PI does not incorporate fuel consumption explicitly, yet acts very effectively in minimizing fuel used. There is a strong link between rate of fuel expenditure $|\dot{m}|$ and $(\alpha - \alpha_{\mathrm{tr}})^2$ and $(T - T_{\mathrm{tr}})^2$ penalty terms in the PI. The link arises primarily because $\dot{m} = -(\mathrm{TSFC})T$, where TSFC is thrust specific fuel consumption (assumed constant at 6×10^{-6} kg/s/N), and secondarily because T is closely related to α^2 in the dynamic model [1].

Parameter Q_3 in the CIS score function [1] is the weight assigned to the cumulative mass loss (fuel consumed) as of maneuver completion $|\Delta m_f|$. In [1], Q_3 is 0.3, and in the present work Q_3 values of 0.0, 0.3, and 0.6 have been tested. Results are here presented for $Q_3 = 0.6$, but no significant differences in $|\Delta m_f|$ were found for Q_3 of 0.0 and 0.3, verifying that the PI is a good surrogate for fuel consumed.

The trajectories for methods A and B start with the vehicle in horizontal flight trimmed for minimum steady-state thrust required (via iteration of the trim functions listed for method A in Table 1). Powered ascent trajectories start at an altitude h of 2000 m, with $\alpha_{\mathrm{tr}_0} = 5.252$ deg, $V_{\mathrm{tr}_0} = 70.99$ m/s, $T_{\mathrm{tr}_0} = 4464$ N (455.2 kgf), and $m_0 = 2500$ kg. Powered descent trajectories start at an altitude of 6000 m, with $\alpha_{\mathrm{tr}_0} = 5.252$ deg, $V_{\mathrm{tr}_0} = 87.69$ m/s, $T_{\mathrm{tr}_0} = 4464$ N, and $m_0 = 2500$ kg (α_{tr_0} and T_{tr_0} do not change with altitude because $V_{\min}$ is adjusted in accordance with Table 1). As in [1], methods A and B allot an initial flight interval of 5.0 s for in-flight costate initialization; accordingly, the powered maneuvers begin at $t_0 + 5.0$ s. The final horizontal position x_f and final horizontal velocity are free for methods A and B in these simulations. The solution is subject to pathwise inequality constraints, including minimum V of 30 m/s, maximum $|\dot{\alpha}|$ of 2.0 deg/s, maximum $|\dot{T}|$ of 1000 N/s, minimum T of 2000 N, and maximum T of 20,000 N. The minimum thrust constraint is very significant in powered descents.

Results for methods A and B are presented in Fig. 1 and Table 2. All trajectories shown have final altitude errors of less than 1.0 m and final altitude-rate errors of less than 0.1 m/s, thereby satisfying the specified final-value accuracy requirements. Figure 1 presents altitude vs horizontal distance profiles for the best performance (minimum fuel expenditure) 600, 900, and 1200 s ascents and descents. Table 2 lists fuel expenditure vs maneuver duration for the trajectories presented in the figure, followed by median fuel expenditure of the numerous acceptable solutions computed for the indicated cases.

The table shows that method A uses less fuel for all maneuvers, although methods A and B are nearly equal for 900 and 1200 s ascents. On average, method A uses 14.70% less fuel than method B. The A'_d entry in Table 2 shows that the best 900 s descent *noncontrary* mode uses 21.62 kg of fuel; whereas the *contrary* solution uses only 16.58 kg (23.3% less). The dashed line curve in Fig. 1 shows the altitude profile of the noncontrary solution A'_d to compare with the A_d solution for 900 s descent.

Statistical performance of the CIS can be analyzed in part by considering both the probability p_c of convergence to a costate vector that produces acceptable final accuracies and a smoothness conditional probability p_s that a solution that is acceptable in terms of final-state accuracies also has no midcourse CRA acceleration rates of change greater than 0.1 m/s^3. Using $Q_3 = 0.6$, method A exhibits probabilities $p_c = 0.42$ and $p_s = 0.75$, giving joint probability 0.32; whereas for method B, $p_c = 0.82$ and $p_s = 0.99$, giving joint probability 0.81. Therefore, the search efficiency of the CIS using method B is more than twice that for method A, so method B may be better suited for online guidance than method A, although the latter provides superior fuel economy.

IV. Simulation Results for Method C (Glide)

The third trim-reference formulation, method C, suitable for glide weapons, provides independent governance over impact position and final descent (strike) angle. Any specified strike angle between $\gamma_f = 0$ and $\gamma_f = -180$ deg, including a vertical strike, can be produced within a large footprint of achievable impact positions. For method C, the α penalty in the PI uses the trim reference associated with maximum steady-state glide range, which is, assuming that α is small [2],

$$\alpha_{\mathrm{tr}} = \sqrt{C_A/(C_{N_\alpha} - C_A)} \tag{17}$$

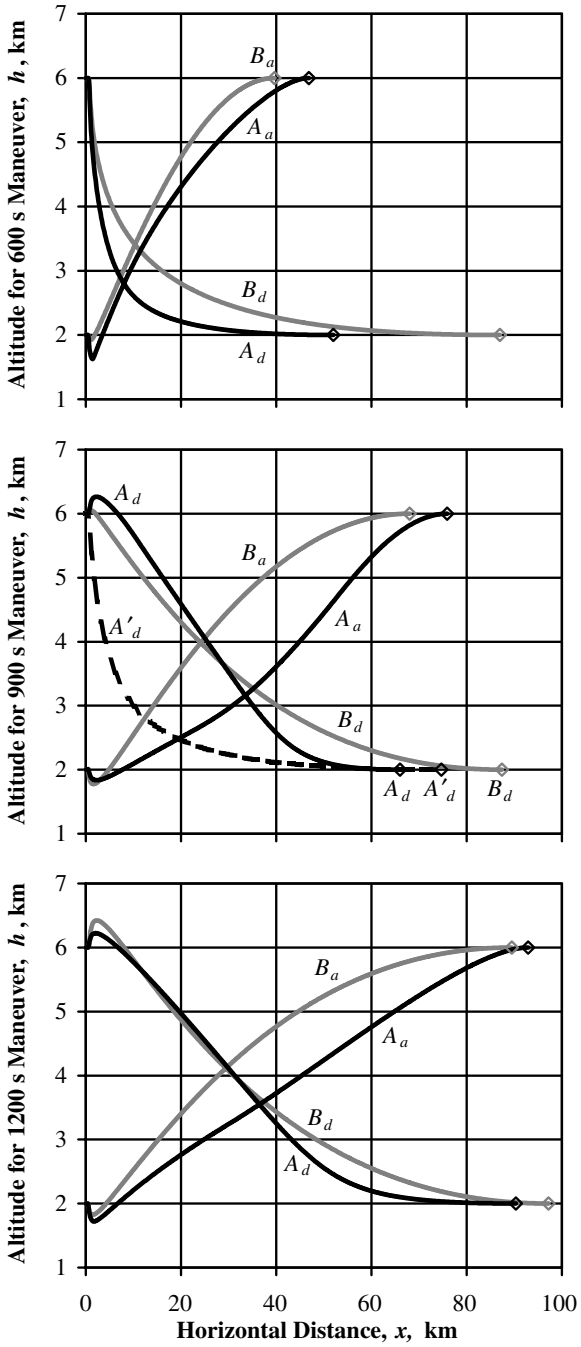

Fig. 1 Altitude profiles for method A ascent A_a and descent A_d and for method B ascent B_a and descent B_d maneuvers. Dashed curve pertains to noncontrary maneuver A'_d having high fuel consumption.

Table 2 Best and median fuel expenditure, kg, for trajectories shown in Fig. 1

Type	Maneuver duration, s					
	600		900		1200	
A_a	c[a]	23.70/23.97	c	31.67/31.80	c	39.72/39.75
A_d	nc	13.98/15.36	c	16.58/19.30	c	24.64/29.35
A'_d	——	——	nc	21.62	——	——
B_a	c	25.77/26.14	c	32.12/34.21	c	40.38/42.32
B_d	nc	31.08/31.18	c	22.26/23.29	c	26.06/29.32

[a]c is contrary maneuver, nc is noncontrary maneuver.

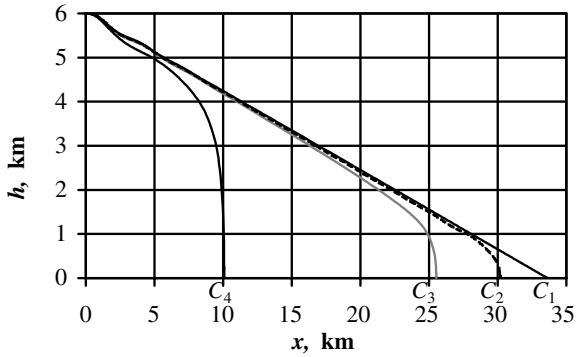

Fig. 2 Altitude profiles for representative glide trajectories.

Figure 2 and Table 3 present results for representative glide trajectories.

For method C (glide) trajectories, α_{tr_0} at 6000 m altitude is nominally 5.252 deg and V_{tr_0} is nominally 87.69 m/s, except for the C_5 trajectory initiated with a perturbed V_{tr_0} of 97.69 m/s. In the glide simulations, $T = T_{tr} = 0$ and vehicle mass is constant at $m =$ 2500 kg. The steady-state glide angle and speed (phugoid-mode equilibrium values) associated with α_{tr} from Eq. (17) are, assuming α is small,

$$\gamma_{ss} = -\tan^{-1}\left[\frac{C_1 + C_2\alpha_{tr}^2}{(C_2 - C_1)\alpha_{tr}}\right] \tag{18}$$

$$V_{ss} = \sqrt{mg/\rho}\Big/\sqrt{[(C_2 - C_1)\cos\gamma_{ss} - \alpha_{tr}C_2\sin\gamma_{ss}]\alpha_{tr} - C_1\sin\gamma_{ss}} \tag{19}$$

Trajectories $C_1, \ldots, C_4$ in Fig. 2 and Table 3 begin with the same velocity ($V_{min} = 87.69$ m/s) and subsequently glide along paths determined by $\lambda_2(t)$ and λ_3, because the other costates ($\lambda_1, \lambda_4, \lambda_5$) are set everywhere to zero for this example. λ_3 is always constant [1]. Trajectory C_1 is the null-costate path, in which $\alpha(t)$ is constant at 5.252 deg and the phugoid steady-state velocity decreases as ρ increases. C_1 is the maximum-range glide, with impact at $x_f = 33,618$ m; $\gamma_f = \gamma_{ss} = -10.24$ deg; $V_f = 64.4$ m/s. Trajectories C_2, C_3, C_4 use λ_{2_0} and λ_3 values that produce approximately vertical impacts for representative impact positions. One observes from Table 3 that λ_{2_0}, λ_3 combinations exist that produce essentially the same strike angle independent of impact position over an available footprint of approximately 20 km. Trajectory C_5 has impact γ_f and x_f values identical to those of C_4, but starts with a velocity 10 m/s greater; an adjustment of λ_{2_0}, λ_3 is used to compensate for the perturbed C_5 release.

Figure 3 indicates the feasibility of independently establishing desired x_f and γ_f impact states within a large region of achievable impacts. The figure shows isoclines of x_f and γ_f plotted on a field of λ_{2_0}, λ_3. The glide range increases and the impact-angle magnitude decreases as λ_{2_0} and λ_3 decrease. Waviness of the distance and impact-angle contours for small initial costate values is not a numerical artifact but relates to phugoid activity. Impact-angle contours are presented in the figure for −60, −90, and −120 deg. Intersections on the $\gamma_f = -90$ deg isocline that characterize trajectories C_2, C_3, and C_4 are indicated. If desired, the UAV can be

Table 3 Representative glide trajectories

Trajectory	x_f, m	γ_f, deg.	V_f, m/s	V_0, m/s	$\lambda_{2_0} \times 10^5$	$\lambda_3 \times 10^7$
C_1	33,618[a]	−10.24	64.4	87.69	0	0
C_2	30,187	−88.90	113.4	87.69	53.6	0
C_3	25,531	−89.80	149.8	87.69	12	10.7
C_4	10,081	−89.60	205.7	87.69	37	38.8
C_5	10,081	−89.60	206.7	97.69	35.444	41.629

[a]Maximum range

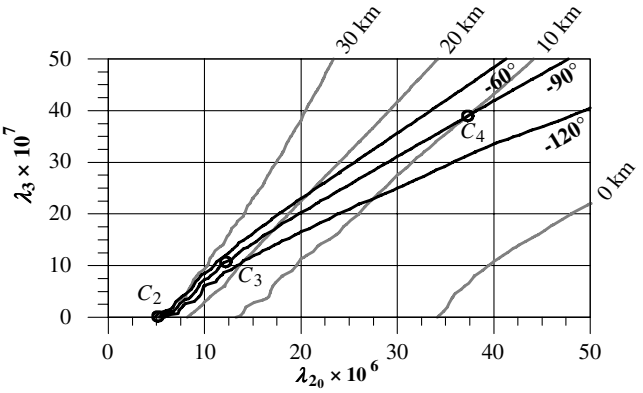

Fig. 3 Costate λ_3 vs initial costate λ_{2_0}. Contours show final downrange distance x_f and final flight-path angle γ_f for glides from $h_0 = 6000$ m, $V_0 = 87.69$ m/s, $\gamma_0 = 0$ to sea-level impact. Circles denote costate initializations for Trajectories C_2, C_3, C_4 in Fig. 2 and Table 3.

guided to reverse its glide heading within a vertical plane to achieve a retrograde attack or landing.

Polynomial networks [3,4] could model approximate values of λ_{2_0} and λ_3 as functions of γ_0, m, x_f, γ_f, and ρ_0 (or h_0), and the CRA could refine estimates provided by such networks.

V. Discussion

The indirect method of [1] and this paper provides $\alpha(t)$ and $T(t)$ solutions for motion of the vehicle along an optimum path to go from measured initial states to desired final states. The trajectory may be generated offline to study system performance. In an online predictive-guidance system, the method requires measured initial states, specified final states, and specified final time at each new point of guidance decision along the maneuver path. The system would use this information in conjunction with its ongoing best estimates of vehicle parameter values for real time computation of $\alpha(t)$ and $T(t)$ commands transmitted to their feedback-control loops. This could be viewed as a realization of optimum, shrinking-horizon guidance having reconfiguration capability.

Computational burden of the improved indirect method is determined principally by the required number of independent threads and allowable number of iterations per thread within the costate initialization search. This burden is least for the glide-weapon trim reference and greatest when using the trim-reference functions derived for minimum time-varying equilibrium thrust.

An air vehicle might be tasked during a mission to A) cruise and loiter for long duration using as little fuel as possible during altitude changes, B) change altitude efficiently yet avoid what is here termed "contrary" altitude behavior when maneuvering close to terrain, and C) perform as a glide weapon. The three trim-reference functions analyzed in this paper correspond to such mission segments. Other applications for the same or similar trim-reference functions can be visualized, and, although there are no universal trim-reference functions, it is believed that this Note will suggest approaches for a variety of air-vehicle types and missions.

VI. Conclusions

Trajectory optimization involving trim-reference functions determines time-varying increments to nonsteady, static-equilibrium trim references. These increments satisfy trajectory boundary requirements in a manner that extremizes a related maneuver-cost functional. An improved indirect method for air-vehicle TPBV trajectory optimization, based upon trim-reference functions for motion within a vertical plane, is extended and analyzed herein. Simulation results are presented that demonstrate 1) a potential for significant fuel savings in powered TPBV ascent and descent maneuvers and 2) an approach to glide-weapon trajectory optimization and guidance that realizes independently specifiable glide range and impact angle (for shallow, vertical, and retrograde impacts) in a large region of realizable impact points.

References

[1] Barron, R. L., and Chick, C. M., III, "Improved Indirect Method for Air-Vehicle Trajectory Optimization," *Journal of Guidance, Control, and Dynamics*, Vol. 29, No. 3, 2006, pp. 643–652.

[2] Barron, R. L., "Trigonometric Models for Large-Angle Aerodynamic Force Coefficients," *Journal of Guidance, Control, and Dynamics*, Vol. 26, No. 5, 2003, pp. 825–827.

[3] Barron, A. R., and Barron, R. L., "Statistical Learning Networks: A Unifying View," *Proceedings of the 20th Symposium on the Interface, Computing Science and Statistics*, edited by E. Wegman, American Statistical Association, Alexandria, VA, 1998, pp. 192–203.

[4] Ward, D., "Generalized Networks for Complex Function Modeling," *Proceedings of IEEE Systems, Man, and Cybernetics Conference*, Institute of Electrical and Electronics Engineers, Piscataway, NJ, 1994.